World Applied Sciences Journal 13 (6): 1302-1309, 2011
ISSN 1818-4952

Transmission Performance of Coded Orthogonal Frequency Division Multiplexing for Radio over Multimode Fibre Systems

[1]Aser M. Matarneh and [2]Nidal A. Al-Dmour

[1]Department of Elecrical Engineering, Mutah University, 61710, Jordan
[2]Department of Computer Engineering, Mutah University, 61710, Jordan

Abstract: In this paper, a performance evaluation of radio over multimode fibre system (ROMMF) using Coded orthogonal frequency division multiplexing (COFDM) is presented. The performance analyses based on bit-error ratio (BER) are extensively investigated. In addition, the effect of fibre length on BER performance is presented. Moreover, the effect of the exponent refractive index profile of the multimode fibre (MMF) on the BER of COFDM is studied considering Maximum Likelihood Ratio (MLR) and sub-optimal simplified Log Likelihood Ratio (LLR) as a soft bit metrics for soft decision Viterbi decoding.

Key words: Bit error rate · Coded-orthogonal frequency division multiplexing · Multimode fibre · Radio over Multimode fibre · Transfer function

INTRODUCTION

The radio over fibre technology (ROF) has been revolutionized to meet the huge demands of high capacity and high purity of broadband services. The ROF technology has been known to have a number of advantages such as transparency to any modulation technique, relatively low attenuation loss, a good potential for cost and large affordable bandwidth. These features have made ROF an attractive solution for fourth generation communication networks (4G) [1]. Particularly, radio over multimode fibre system (ROMMF) has gained much attention recently for its suitability to deliver high purity signals in analogue and digital format for short- reach coverage such as wireless local area networks (WLANs) and ultra-wideband (UWB) radio signals [2].

A considerable attention has been paid to orthogonal frequency division multiplexing (OFDM) which has already been employed in digital audio broadcasting (DAB), high definition TV (HDTV) and ROF technology and many other examples. Since OFDM is widely used today in many applications, it is one of the preferable modulation schemes for next generation systems. In ROF, OFDM impact has been demonstrated with multimode fibre (MMF) as a promising modulation scheme for mitigating the modal dispersion penalty [3]. Having a high spectral efficiency, OFDM can efficiently utilize the system bandwidth (for 64 subcarriers, the spectral efficiency can reach 1.98 Bd/Hz) [4]. OFDM is inherently able to transfer a frequency selective fading channel into a number of flat fading sub-channels. However, inserting cyclic prefix between subcarriers relaxes the intersymbol interference (ISI) which can destroy the orthogonality among subcarriers. This is achieved by setting the carrier spacing and reciprocal of the symbol period to be equal [5]. By implementing coding and interleaving across sub-carriers, the effect of multipath-fading is minimized since interleaving reorganizes the number of bits in such away to avoid the effects of fading. Convolutional coding is being used commonly in OFDM systems and it can give coding gain at different coding rates [4, 6]. Thus, coded-OFDM (COFDM) makes the transmitted signal robust to multipath fading and distortion.

MMF has a merit of being used for short distance applications; it is typically a popular choice for in-building networks. MMF possesses a large core diameter (> 50μm) leading to better coupling efficiency with an optical source and enabling low cost electro-optic devices that can be adopted in the ROMMF system such as VCSEL [7, 8]. In addition, it is cheaper than single mode fibre (SMF) since it has lower installation and maintenance costs. Thus, a wide selection of services with different signal characteristics such as Fast Ethernet, Gbit Ethernet,

Corresponding Author: Nidal A. Al-Dmour, Department of Computer Engineering, Mutah University, 61710, Jordan. Tel: +96-27050705, E-mail: nidal@mutah.edu.jo.

video, audio and control signals are likely to be supported by MMF within a range of a few kilometers. As a low cost route, MMF is an attractive and cost-effective solution for transporting multiple services. However, the signal propagation through MMF is subject to significant signal impairment leading to both attenuation and time spread of the transmitted signal. The latter is caused basically by material dispersion and modal dispersion. Dispersion causes pulse broadening as the pulse propagates along the fibre which limits the information carrying capacity of an optical fibre and is determined by bandwidth-distance product which typically is measured in (MHz.Km). In contrast to SMF, modal dispersion exists in MMF due to the large number of fibre modes being propagated inside the core of MMF.

The research effort towards modelling of ROF using OFDM and electro-optic modulator has been recently reported [9] using single mode fibre. On the other hand, interesting and useful study of the transmitting OFDM over MMF will be mandatory since dispersion and losses are the main limiting factors. In this letter, a comprehensive modelling study of OFDM transmission over MMF is presented. In the context of this work, the dispersion and losses of MMF have been accurately taken into account by adopting the transfer function model of MMF proposed in [10]. It is an analytical model which can be easily incorporated into the system model and accurately consider the mode coupling effect of MMF (MC) and the differential mode attenuation (DMA). Moreover, the effect of fibre length and the exponent refractive index profile (α) have been investigated. The theoretical findings of the modelling study have also been supported by measurements taken from our experimental setup of this system. This study, to the best of the authors' knowledge, is the first study which takes into account the MC and the DMA for the performance analysis of ROMMF system employing COFDM. The performance analyses in terms of BER analyses are discussed in detail. Furthermore, the measured MMF response for various lengths is included in the analysis for BER simulation.

COFDM Model: The time domain representation of OFDM signal can be defined as [9]

$$s(t) = \mathrm{Re}\left\{\sum_{i=-n/2}^{i=(n/2)+1} d_i(t) e^{\left(2j\pi(f_0 - f_i)t\right)}\right\} \qquad (1)$$

Where n denotes the inverse fast Fourier transform (IFFT) window size, f_0 is the central frequency, f_i is the frequency of ith subcarrier, d_i represents the complex digital symbols and i denotes the index of the complex digital symbol.

The implementation process of COFDM is as follows:

- The data bits are convolutionally encoded with a code rate ½.
- The encoded bits are bit-interleaved and then mapped into in-phase and quadrature components of the complex symbol using Gray-coded mappings.
- The complex symbols are modulated by OFDM as in Eq. (1).
- The MMF channel is assumed to be stationary channel for, at least, transmission of one COFDM symbol. Although such an assumption holds for fibre, it is not normally valid for the RF channel. Also, the noise is assumed to be a complex additive white Gaussian noise (AWGN).
- At the receiver, for coherent detection, each modulation symbol could be recovered by conventional equalization referred to as one-tap frequency domain equalizer [11]. Table 1 summarizes COFDM parameters.
- The decoding process employs the soft-decision Viterbi decoding algorithm which involves either Maximum Likelihood Ratio (MLR) or simplified Log Likelihood Ratio (LLR) as soft-bit metrics.

In the following analysis, both quadrature phase shift keying (QPSK) and quadrature amplitude modulation (QAM) are used to modulate the COFDM subcarriers for the BER simulation.

The superiority of Convolutional coding with Soft/Hard-Viterbi decoding effect is shown in Fig. 1, uncoded QPSK-OFDM is added for comparison. The number of subcarriers is 64 and the data rate is 12 Mbps. It can be seen that using soft decoding enhances the required E_b/N_0 for particular BER. Example of this can be readily seen at BER equal to 10^{-5}. Around 2 dB improvements are achieved by soft decision Viterbi decoding over hard decision Viterbi decoding.

MMF Response Model: The block diagram of the ROMMF system used for analysis and simulation is shown in Fig. 2. In this system the COFDM signal generated out of the OFDM transmitter at the carrier frequency using Eq. (1) was directly injected into the laser diode (LD) at desired signal level with dc-biasing that is well above the laser threshold.

Table 1: COFDM parameters

Parameter	Value
Code rate	1/2
Generator polynomials	133_8
	171_8
Constraint length	7
Number of OFDM data subcarriers (N_c)	200
Subcarrier spacing	0.84 MHz

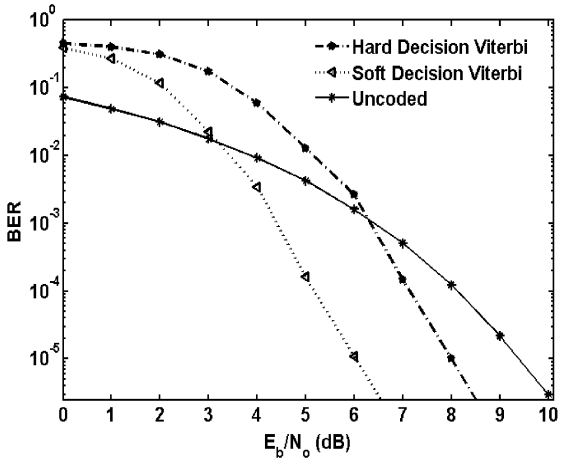

Fig. 1: BER of QPSK-OFDM with uncoded, Convolutional coding, hard and soft decision Viterbi detection. N_c=64, data rate =12 Mbps.

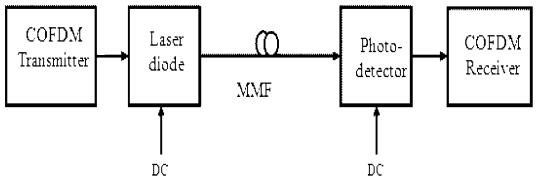

Fig. 2: Demonstration of ROMMF system under intensity modulation and direct detection

The optical intensity signal out of the laser diode is fed into a MMF followed by a photodetector(PD). The received COFDM signal will be equalized, demodulated and decoded to get back the data. This system can be used for analyzing the performance of the optical link alone for the OFDM input.

The RF transfer function of the MMF system has been given in [10, 12] based on the electric field propagation through MMF.

$$H(\omega)=\sqrt{1+a_c^2}\; e^{\frac{-1}{2}\left(\frac{\beta^2_0(\omega Z)}{\sigma_c}\right)^2} Cos\left(\frac{\beta^2_0\omega^2 Z}{2}+arctan(a_c)\right) \sum_{v=1}^{M} 2v\left(C_{vv}+G_{vv}\right) e^{-2\alpha vZ}\, e^{-j\omega\tau_v} \quad (2)$$

Where, Z is the fibre length and β_0^2 is the second-order chromatic dispersion parameter which is equivalent to the second derivative of the propagation constant β_v and is assumed to be equal for all the fibre modes. α_v is the fibre attenuation and α_v is the chirp parameter, ω_v is RF angular modulation frequency, $\sigma_c \approx 1/(\sqrt{2}\,W)$ is the optical source RMS coherence time and W is the source RMS linewidth, it is assumed that an optical source has a finite linewidth spectrum with a Gaussian time domain autocorrelation function, v is the mode group number, C_{vv} and G_{vv} are coupling and uncoupling fibre mode coefficients, respectively, their equations can be found in [10] and τ_v is the group delay corresponds to v-group.

Intermodal dispersion is a result of time delay difference among guided modes. Each mode propagates with a different group velocity. Therefore, the higher the group delay difference, the higher the pulse spreading. Pulse spreading increases the effective channel delay, which leads to so-called modal dispersion. However, this kind of distortion is not present in SMF while it is significant in the MMF.

The group delay, the delay time of the guided modes, is calculated from the propagation constant β_v [1, 13].

$$\tau(v,\lambda)=\frac{\partial\beta_v}{\partial\omega}$$

and therefore

$$\tau(v,\lambda)=\frac{N_1(\lambda)}{c}\left[1-\frac{\Delta(\lambda)(4+\varepsilon(\lambda))}{\alpha+2}\right]^{\frac{2\alpha}{\alpha+2}}\left[1-2\Delta(\lambda)\left(\frac{v}{M}\right)^{\frac{2\alpha}{\alpha+2}}\right]^{-1/2} \quad (3)$$

Where λ is the wavelength, c is the velocity of light in vacuum and ε is the profile dispersion parameter given by [13]

$$e(\lambda)=-\frac{2\,n_1}{N_1}\frac{\lambda}{\Delta}\frac{\partial\Delta}{\partial\lambda} \quad (4)$$

Δ is the refractive index contrast between the core center (η_1) and the cladding (η_2) and it is given by

$$\Delta=\frac{n_1-n_2}{n_1} \quad (5)$$

N_1 is the material group index defined as [14]

$$N_1(\lambda)=n_1-\lambda\,\frac{\partial n_1}{\partial\lambda} \quad (6)$$

M is the number of mode groups propagating along the fibre and is given by

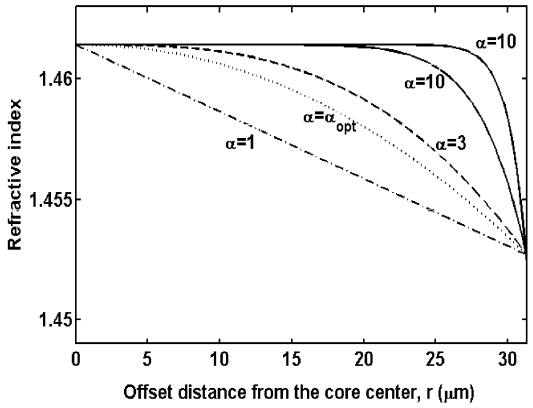

Fig. 3: Refractive index profile for 62.5/125 μmMMF, n_1= 1.46143, n_2 = 1.45274, Δ = 0.00595 and λ= 850 nm.

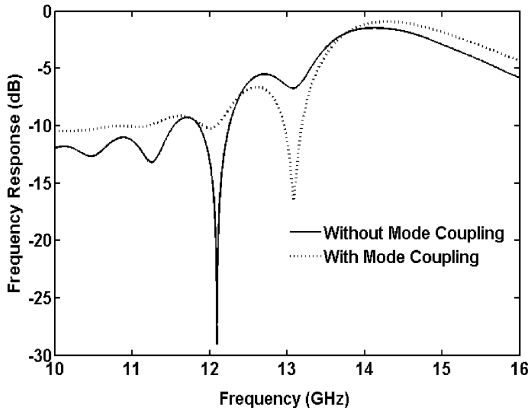

Fig. 4: Effect of Mode Coupling (MC) on the transfer function of GI-MMF link for λ= 850 nm, Z= 2014 m, α=2

$$M(\alpha,\lambda) = 2\pi\ a\frac{n_1(\lambda)}{\lambda}\left[\frac{\alpha\ \Delta(\lambda)}{\alpha+2}\right]^{1/2} \quad (7)$$

Where a is the core radius and α is the exponent refractive index profile ($\alpha > 0$).

The minimum modal dispersion of MMF occurs at the optimum α which can be obtained by [13]

$$\alpha_{opt} = 2+\varepsilon-\Delta\ \frac{(4+\varepsilon)\ (3+\varepsilon)}{5+2\varepsilon} \quad (8)$$

The above relation shows that α_{opt} depends on Δ and ε and eventually on the wavelength. Because the modal dispersion is at minimum at α_{opt}, the largest achievable 3-dB bandwidth can be obtained at α_{opt}. Fig. 3 illustrates the effect of α profile of graded index MMF (GI-MMF). It can be noted that iα controls the profile shape of the refractive index. When α =2, the core profile exhibits a parabolic shape. Nevertheless, by increasing α, the core profile becomes gradually uniform and converges to the step-index profile for large values of α ($\alpha > 25$).

However, in the presence of different sources of loss in MMF, additional loss comes from mode-interactions between at least two adjacent modes within the core area, thus, the attenuation coefficient differs from mode to mode according to an empirical formula suggested in [10, 15].

$$\alpha(v,\lambda) = \alpha_0(\lambda) + \alpha_0(\lambda)\ I_p\left[\eta\left(\frac{v-1}{M}\right)^{\frac{2\alpha}{\alpha+2}}\right] \quad (9)$$

Where α_0 is the intrinsic fibre attenuation, I_p is the ρth-order modified Bessel function of the first kind and η is a weighting constant.

The function of differential mode attenuation (DMA) is to highly attenuate higher order modes (the modes that propagate away from core center) and their effects on the overall fibre response are eliminated, leaving stronger modes to represent the multimode fibre response. Only low-order modes will arrive at the other end of fibre with different group delay.

It should be mentioned that the evaluation of the refractive index of optical fibre material is well-approximated by the Sellmeier equation [16]. By evaluating the refractive indices n_1 and n_2 for λ= 850 nm, the propagation constant (β_v) and wavelength-dependent parameters as well as mode-dependent parameters can be calculated. Table 2 presents these parameters which have been used in the simulation of MMF transfer function.

The investigation of the MC effect on the transfer function of the MMF link is shown in Fig. 4. It is worth noting that the 3-dB bandwidth in the presence of MC is ~780 MHz, while in the absence of MC is ~590 MHz.

Table 2: MMF parameters

Parameter	Value
Laser source RMS linewidth	10 MHz
Fibre Dispersion Parameter	-94 ps/(ns.km)
Fibre attenuation (α_0)	1.25 dB/km
Wavelength (λ)	850 nm
Core refractive index (n_1)	1.46143
Clad refractive index (n_2)	1.45274
Material group index (N_1)	1.47517
refractive index contrast (Δ)	0.00595
Profile dispersion parameter (ε)	0.10375
Core diameter (a)	62.5 μm
Laser chirp (α_c)	0
η	7.35
ρ	9

Thus, MC smoothes the link response and increases the 3-dB bandwidth. Moreover, the deep null point located at 12.09 GHz is minimized and shifted to the right when taking into account the MC.

RESULTS

It has been assumed that the maximum delay spread incurred by the channel is shorter than the cyclic prefix of an OFDM symbol. Also, the simulation is carried out on a symbol by symbol basis. Therefore, the cyclic prefix can be dropped out as it has no effect on the BER analysis. It should be noted that no pilot signal is considered for the BER evaluations since perfect channel knowledge is assumed and so, no channel estimation is needed.

Performance results are presented in terms of BER for the QPSK-COFDM and 16-QAM-COFDM systems. The information data bit is encoded with a rate-1/2 convolutional coder. The block interleaver with interleaver depth equal to one OFDM symbol has been selected to exploit the available frequency diversity.

The measured frequency response of MMF is shown in Fig. 5, [17], using lightwave component analyzer (8703A) for 3 m and 800 m fibre length, respectively. The type of MMF is a graded index (GI) with 62.5/125 μm core/clad diameter. The laser source is a vertical cavity surface emitting laser (VCSEL) and directly coupled to the MMF. It can be observed from Fig. 5 that the flat response is shown to appear clearly in the passband region (i.e. beyond 3 dB bandwidth) for 3 m and 800 m fibre, it is therefore possible to transmit multi-channel data at carrier frequencies much greater than the of 3-dB bandwidth of MMF.

The measured MMF response is included in the simulation of BER of QPSK-COFDM system. The number of equally-spaced subcarriers (N_c) is chosen as 200 around the channel center frequency 3 GHz with subcarrier frequency equal to 0.84 MHz and equivalent data rate 168 Mbps. It can be shown from Fig. 6 that for the measured response with 800 m length, E_b/N_0 degrades by more than 1.5 dB than the measured response with 3 m length at BER of 10^{-6}.

The BER performance of MMF at and close to α_{opt} has been evaluated for 5 km of fibre and presented in Fig. 7. Taking the BER=10^{-5}, the required E_b/N_0 is 8.12 dB. However, small deviation from α_{opt} (α_{opt} + 5%) increases the E_b/N_0 to 10.21 dB which results in 2.09 dB penalty in order to achieve the same BER.

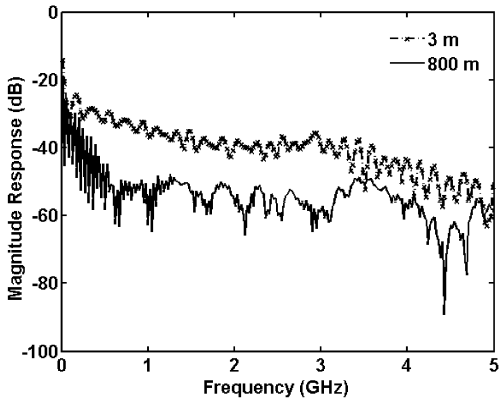

Fig. 5: Measured frequency response for 62.5/125 μm GI-MMF

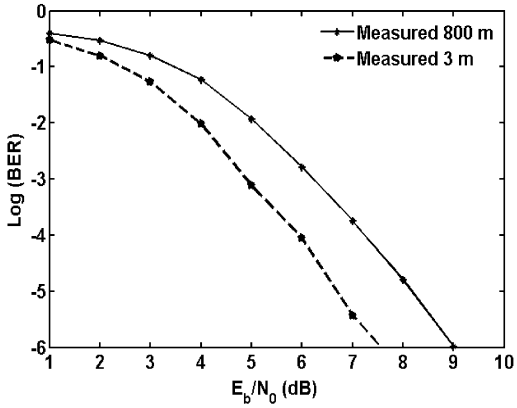

Fig. 6: BER versus E_b/N_0 for QPSK-COFDM transmission over measured MMF response, N_c = 200

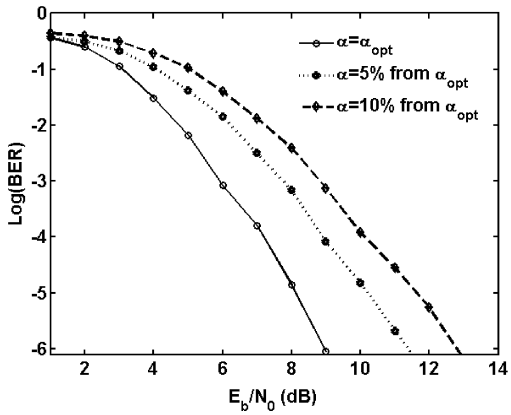

Fig. 7: BER versus E_b/N_0 for QPSK-COFDM transmission over MMF showing the effect of deviation from optimum, N_c = 200, z=5 km.

Moreover, further deviation from α_{opt} (α_{opt} + 10%) necessitates the E_b/N_0 to be around 11.63 dB. Thus, additional penalty by 1.42 dB will be induced to maintain

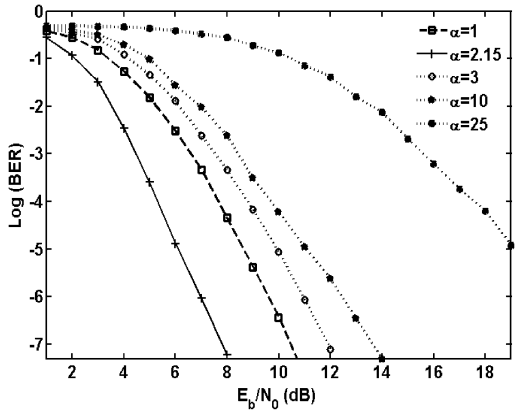

Fig. 8: BER versus E_b/N_0 for QPSK-COFDM with different values of α, z = 2014 m, N_c = 200.

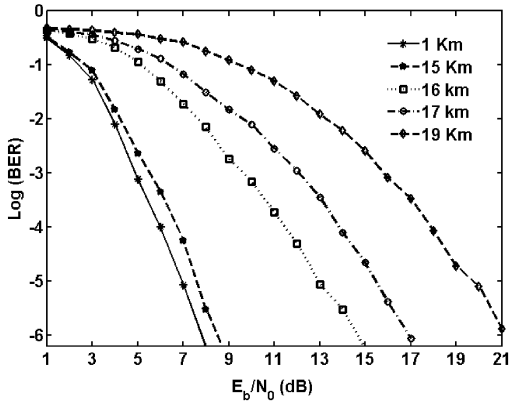

Fig. 9: BER versus E_b/N_0 for QPSK-COFDM with different fibre lengths, α=2.15, N_c = 200

the same BER. As a result, the effect of modal dispersion is considerably reduced by tailoring of the refractive index profile of the fibre. However, the only disadvantage is that it is more expensive than SI-MMF.

According to Eq. (8), the optimum value of α (α_{opt}) for the frequency response at 850 nm wavelength is found to be 2.089, whilst for 1300 nm is 1.9377. It is worth mentioning that at the optimum profile of the refractive index, the delay spread is at minimum leading to the dispersion being at minimum. Fig. 8 depicts the BER evaluations for different values of α. It shows that the BER increases as alpha moves away from its optimum value. Compared with α close to the optimum value (i.e. α=2.15 and α_{opt} = 2.089), around 2 dB is required to achieve the same BER at α =1. As a result, increasing α leads to more degradation of the system performance. By further increase of α (α > 25) the refractive index profile becomes approximately constant and therefore, the fibre tends to be as step-index (SI) mode profile. Consequently, the expense of achieving the required BER becomes higher due to an increase in modal dispersion. It is clear that the best performance is achieved using MMF with α optimum. However, practical MMF is designed and fabricated with nearly parabolic shape (i.e. $\alpha \approx 2$).

The influence of the fibre length on the system performance is displayed in Fig. 9 with N_c equal to 200-COFDM subcarrier spaced equally by 0.84 MHz with and equivalent data rate 168 Mbps and modulated by QPSK. The received signal was equalized by a conventional one-tap frequency domain equalizer. It can be seen that there is no significant degradation of BER until the fibre length becomes close to 15 km due to

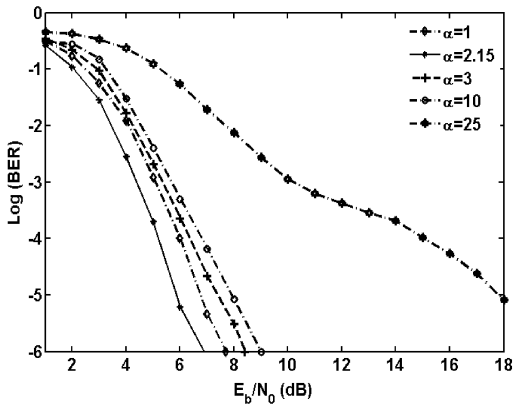

Fig. 10: BER versus E_b/N_0 for QPSK-COFDM using Sub-optimal simplified LLR –Viterbi decoding with different values of α, z = 2014 m, N_c = 200.

the considerable COFDM tolerance of modal dispersion. The degradation is much more pronounced for fibre length longer than 16 km. It thus appears that for fibre length = 16 km the system performance is inferior to that at 1 km fibre length by about 7 dB. After that, the signal distortion cannot be tackled due to the significant increase in modal dispersion and the signal amplification becomes necessary to compensate for losses.

Further simplifications of soft decoding process can be achieved by considering Log Likelihood Ratio (LLR) as a sub-optimal simplified bit metric [11, 18, 19] inside the Viterbi decoder. The advantage of LLR is that, it is more practical for hardware realization than MLR because it relaxes the high computational complexity [11]. To this end, COFDM equalization combined with soft-bit weighting (weighted by square magnitude of channel transfer function) has been considered. Fig. 10 explains that the BER is improved when using soft-bit weighting

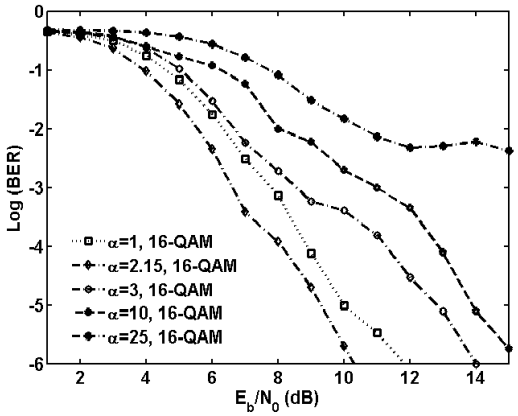

Fig. 11: BER versus E_b/N_0 for 16-QAM-COFDM using Sub-optimal simplified LLR –Viterbi decoding with different values of α, Z = 2014 m, N_c = 200.

Table 3: E_b/N_0 comparison of QPSK for different values of α using sub-optimal simplified LLR –Viterbi decoding and conventional Viterbi decoding, $\log_{10}$ (BER)= -6

	E_b/N_0 (dB)	
α	Soft decision Viterbi decoding of QPSK using MLR	Soft decision Viterbi decoding of QPSK using LLR
1	9.60	7.70
2.15	7.00	6.87
3	10.95	8.40
10	12.45	9.00
25	20.60	19.70

jointly with LLR in the Viterbi decoder. For α=1, around 1.6 dB gain is achieved at BER of 10^{-5} compared with the conventional metric (MLR) used in soft-Viterbi decoder, whereas for α=3 and α=10, the improvement is ~2.5 dB and ~3 dB, respectively. Moreover, E_b/N_0 comparison of QPSK-COFDM for different values of α using optimal simplified LLR–Viterbi decoding and conventional (MLR) Viterbi decoding is included in Table 3 at fixed BER=10^{-6}. It can be observed that no significance difference is found at α=2.15, this can be understood by knowing that the MMF channel effect introduces minimum_distortion at this value of α.

For higher multi-level modulation schemes such as QAM, explicitly 16-QAM, sub-optimal simplified LLR is considered for path metric computation inside Viterbi decoder and the BER results are depicted in Fig. 11. It should be noted that COFDM parameters are considered the same as in the case of QPSK. Therefore, the data rate is doubled for 16-QAM (i.e. 336 Mbps) compared with QPSK.

It is clearly seen from Fig. 11 that the effect of α on the BER is significant, changing α from 2.15 to 3, a penalty of ~ 1.7 dB is induced while for α = 10, results in around 4 dB cost. The BER floor appeared for α = 25 and E_b/N_0 equal to 12 dB as there are no more errors could be corrected with increasing E_b/N_0.

By comparing BER results of QPSK and 16-QAM in Fig. 10 and Fig. 11, QPSK requires less E_b/N_0 than 16-QAM for the same BER. Furthermore, because of its constant amplitude properties, PSK is less susceptible to channel nonlinearities and adds less stringent implementation requirements on the demodulation and recovery of data bits. However, *M*-QAM achieves high levels of spectral efficiency; it turns out that as M increases the advantage of QAM over PSK grows.

CONCLUSIONS

BER evaluation of ROMMF system using COFDM has been presented considering the MC and DMA of GI-MMF. Both the effect of MMF length and the exponent refractive index profile have been taken into account as well as the measured MMF response. The simulation results show that increasing the length of MMF degrades the system performance even though with efficient use of COFDM due to dispersion and losses. However, for short-distance applications, COFDM can be used efficiently for high data rate signal delivery and to tolerate the effect of modal dispersion. Also, the exponent refractive index profile effect has been studied and shown that the best performance can be achieved near the optimum value of exponent refractive index profile. Further work is now under processing to consider an accurate nonlinear laser model into the ROMMF system model and to investigate the overall system performance.

REFERENCES

1. Kim, Y., B.J. Jeong, J. Chung, C.S. Hwang, J.S. Ryu, K.H. Kim and Y.K. Kim, 2003. Beyond 3G: vision, requirements and enabling technologies', IEEE Commun. Mag., 41(3): 120-124.
2. Guennec, Y.L., A. Pizzinat, S. Meyer, B. Charbonnier, P. Lombard, M. Lourdiane, B. Cabon, C. Algani, A.L. Billabert, M. Terré, C. Rumelhard, J.L. Polleux, H. Jacquinot, S. Bories and C. Sillans, 2009. Low-Cost Transparent Radio-Over-Fiber System for In-Building Distribution of UWB Signals, J. Lightwave Technol., 27(14): 2649-2657.

3. Dixon B.J., R.D. Pollard and S Iezekiel, 2001. Orthogonal frequency-division multiplexing in wireless communication systems with multimode fiber feeds', IEEE Trans. Microwave Theory Tech., 49: 1404-1409.
4. Hanzo, L. and T. Keller, 2003. OFDM and MC-CDMA A Primer (IEEE Press/Wiley, 2003).
5. Zou, W.Y. and Y. Wu, 1995. COFDM: an overview', IEEE Trans. on Broadcasting, 41(1): 1-8.
6. Prasad R., 2004. OFDM for Wireless Communication Systems' (Boston: Artech House, 2004).
7. Das, A., A. Nkansah, N.J. Gomes, I.J. Garcia, J.C. Batchelor and D. Wake, 2006. Design of low-cost multimode fiber-fed indoor wireless networks', IEEE Trans. Microwave Theory Tech., 54(8): 3426- 3432.
8. Gomes, N.J., A. Nkansah and D. Wake, 2008. Radio-Over-MMF Techniques–Part I: RF to Microwave Frequency Systems, J. Lightwave Technol., 26(15): 2388-2395.
9. Song, J.B. and A.H.M.R. Islam, 2008. Distortion of OFDM Signals on Radio-Over-Fiber Links Integrated With an RF Amplifier and Active/Passive Electroabsorption Modulators, J. Lightwave Technol., 26(5): 467-477.
10. Gasulla, I. and J. Capmany, 2006. Transfer function of multimode fiber links using an electric field propagation model: Application to Radio over Fibre systems, Opt. Express, 14(20): 9051-9070.
11. Tosato, F. and P. Bisaglia, 2002. Simplified Soft-Output Demapper for Binary Interleaved COFDM with Application to HIPERLAN/2, IEEE International Conference on Communications, ICC 2: 664- 668.
12. Gasulla, I. and J. Capmany, 2007. Transfer function of radio over fiber multimode fiber optic links considering third-order dispersion, Opt. Express, 15(17): 10591-10596.
13. Yabre, G., 2000. Theoretical Investigation on the Dispersion of Graded-Index Polymer Optical Fibers, J. Lightwave Technol., 18(6): 869-877.
14. Yabre, G., 2000. Comprehensive Theory of Dispersion in Graded-Index Optical Fibers, J. Lightwave Technol., 18(2): 166-177.
15. Yabre. G., 2000. Influence of Core Diameter on the 3-dB Bandwidth of Graded-Index Optical Fibers, J. Lightwave Technol., 18(5): 668-676.
16. Agrawal, G.P., 2002. Fiber-Optic Communication Systems (Wiley series in Microwave and Optical Engineering, 2002).
17. Matarneh, A.M., S.S.A. Obayya and I.D. Robertson, 2008. Coded Orthogonal Frequency Division Multiplexing (COFDM) Transmission over Graded-Index Multimode Fiber, IEEE Conference PhotonicsGlobal@Singapore Singapore 2008.
18. Simon, M.K. and R.. Annavajjala, 2005. On the Optimality of Bit Detection of Certain Digital Modulations IEEE Trans. on Commun., 53(2): 299-307.
19. Wang, M.M., W. Xiao and T. Brown, 2002. Soft Decision Metric Generation for QAM With Channel Estimation Error, IEEE Trans. Commun., 50(7): 1058-1061.